Chemical weathering rates in granitic mountain catchments over 10-year and 10, 000 year timescales

RMRS-99604-RJVA

Chemical weathering rates in granitic mountain catchments over 10-year and 10,000-year timescales

Final project report, Research Joint Venture Agreement RMRS-99604-RJVA

James W. Kirchner, Principal Investigator

Introduction

Chemical weathering is the ultimate long-term sink for atmospheric CO_2, the ultimate source for many solutes in stream water, and the ultimate regulator of soil formation rates. At the Silver Creek Experimental Watershed in central Idaho, we have compared measurements of chemical weathering rates over 10-year and 10,000-year timescales. The decade-scale weathering rates are derived from catchment mass balances of bulk deposition and streamflow losses [*Clayton and Megahan*, 1986], and the 10,000-year measurements are derived from a new method [*Riebe et al.*, 2001] combining X-ray fluorescence measurements of rock and soil chemistry and cosmogenic nuclide measurements of long-term rates of denudation [*Kirchner et al.*, 2001].

Cosmogenic nuclides are produced inside mineral grains by cosmic rays bombarding the Earth's surface. Because cosmic ray intensity decreases rapidly with depth (due to shielding by the overlying material), the concentration of cosmogenic nuclides in minerals indirectly records the length of time that those minerals have been close to the Earth's surface, and thus records their average erosion rate. The surface lowering rate can be directly calculated from the cosmogenic nuclide concentration in minerals reaching the surface, via the formula $E=P_0\Lambda/N$ [*Lal*, 1991], where E is the surface lowering rate, N is the isotope concentration, P_0 is the nuclide production rate at the surface and Λ is the absorption mean free path ($\Lambda\approx60$ cm in rock). The nuclide concentration N averages the erosion rate over a time scale of order Λ/E, the time required to remove a layer of thickness Λ from the surface ($\Lambda/E\approx1{,}000$'s of years for typical temperate-zone erosion rates). Because cosmogenic nuclide concentrations reflect average erosion rates over thousand-year timescales, they are insensitive to recent changes in erosion rates. This makes them particularly useful for estimating long-term "background" rates of erosion, for comparison with modern-day erosion rates.

We have recently used cosmogenic nuclides (^{10}Be and ^{26}Al) in stream sediment to measure catchment-scale denudation rates over 10,000-year timescales at 32 unglaciated granitic watersheds in central Idaho [*Kirchner et al.*, 2001], including 6 catchments at Silver Creek. At these same watersheds, sediment yields have also been measured by sediment trapping or sediment gauging over shorter timescales (4-84 yr, mean=23). Our original aim was to test whether the cosmogenic measurements could

212. Kirchner, James W. *Chemical weathering rates in granitic mountain catchments over 10 year and 10,000 year timescales.* [2001?]: 16 p. [Unpublished RMRS cooperative agreement ; 99-604-RJVA]

be used as "benchmarks" for measuring the erosional consequences of land use [e.g., *Brown et al.*, 1998]. To our surprise, however, at every site long-term denudation rates measured by cosmogenic nuclides were about a factor of 20 greater than shorter-term erosion rates measured from sediment yields. This discrepancy between short-term and long-term erosion rates was consistent across watersheds ranging over five orders of magnitude in size, from small experimental watersheds to the entire Salmon River drainage. Methodological differences cannot explain the mismatch between short-term and long-term erosion rates, nor can climatic changes. Instead, we hypothesized that in the mountains of central Idaho, long-term average erosion rates are dominated by catastrophic erosion events that are too rare to be reliably observed in typical sediment yield studies. For example, one of our sites was monitored with sediment traps for 25 years, but the total sediment yield over this entire period was dwarfed (by more than 10-fold) by a single debris flow several years later. These observations suggest that mountain erosion and sediment delivery to streams may be extremely episodic, and may subject aquatic ecosystems to catastrophic disturbance.

Comparing long-term and present-day rates of chemical weathering in Idaho watersheds

The observed discrepancy between short-term and long-term erosion rates at our Idaho study sites naturally raises the question of whether there is a similar mismatch between short-term and long-term rates of chemical weathering. Intuitively, one would expect that chemical weathering should be much less episodic than physical erosion, but this needs to be verified. To test this hypothesis, we are employing a new method for inferring long-term rates of chemical weathering from cosmogenic nuclide measurements. We have applied this method at three Silver Creek watersheds, Dee Creek (SC-2), Cabin Creek (SC-5), and Control Creek (SC-6). At all three watersheds, present-day chemical weathering fluxes have already been measured from mass balances of chemical inputs in precipitation and chemical outputs in streamflow [*Clayton and Megahan*, 1986].

Our method for estimating long-term chemical weathering rates at these sites is an extension of soil mass balance methods [*April et al.*, 1986; *Brimhall et al.*, 1992; *White et al.*, 1998], which have traditionally been applicable only to un-eroded soil deposits whose age and initial composition are known. Using cosmogenic nuclide measurements of total denudation rates, we can extend these methods to soils undergoing steady-state erosion. If soils are in erosional steady state then over the long term, bedrock must be converted to soil at a rate equal to the long-term denudation rate D, which we can measure for whole watersheds using the cosmogenic nuclide techniques described above. In erosional steady state, conservation of mass requires that the solute flux of any element (here, Ca) from chemical weathering must equal the balance between the element flux from bedrock conversion to soil, and the element flux from physical erosion of soil, or

$$W_{Ca} = D \{ [Ca]_{rock} - [Ca]_{soil} [Zr]_{rock}/[Zr]_{soil} \} \quad (1)$$

Where W_{Ca} is the chemical weathering flux of Ca, D is the total denudation rate (the sum of physical erosion and chemical weathering, in T km^{-2} yr^{-1}), and $[Ca]_{rock}$ and $[Ca]_{soil}$ are the average concentrations (ppm by mass) of Ca in bedrock and soil. The ratio $[Zr]_{rock}/[Zr]_{soil}$ corrects for the loss of mass as rock is converted to soil. Because Zr is extremely insoluble, its concentrations in parent bedrock and soil indicate how much bedrock was the parent material for a given mass of soil. Other immobile elements can also be used for this purpose; we are testing this mass balance method using Zr, Th, Nb, Y, and Ti. Summing equation 1 over all the rock-forming elements, we can calculate the total rate of chemical weathering (mass per unit area per unit time) as

$$W_{Total} = D \{ 1 - [Zr]_{rock}/[Zr]_{soil} \} \quad (2)$$

and conversely, we can calculate the rate of mass removal by physical erosion as

$$E_{Physical} = D \{ [Zr]_{rock}/[Zr]_{soil} \} \quad (3)$$

These mass balance principles allow us to estimate chemical weathering rates over the same timescale that cosmogenic nuclides measure total denudation rates (i.e., the time required to erode the surface by $\Lambda \approx 60$ cm, which is 5,000-12,000 years at the Silver Creek catchments).

Field sampling

We collected 411 samples (257 samples of soil and 154 samples of bedrock and saprolite) from the three Silver Creek study catchments. Quality-control samples and samples taken from surrounding rock outcrops bring the total number of samples analyzed to 463. Sampling locations were dispersed throughout the study catchments, with irregular but roughly even spacing between sampling points.

Soil samples made up nearly two-thirds of the total sample count (Table 1), with three-quarters of the soil samples being grab samples of the soil surface or A horizon samples from soil pits. Soils in the study catchments were thin and often lacked clear horizon structure; as a result, many of the soil pits were shallow and resulted in only a single A horizon sample. In pits where horizons were discernible, each horizon was sampled individually.

Just over one-third of the samples taken were parent material (rock or saprolite), with roughly half of these coming from bedrock outcrops, and the other half coming from saprolite from the bottom of soil pits or from rock fragments incorporated in the soil matrix. For almost all of the elements analyzed, the average concentrations in bedrock outcrops were not statistically distinguishable from those in saprolite or rock fragments.

Table 1. Sample counts for geochemical analyses

	SC-2	SC-5	SC-6	Total
Sampling locations	55	107	133	295
Soil pits	51	19	19	89
Soil samples	53	84	120	257
of which surface samples or A horizon	44	62	84	190
Parent material samples	56	51	47	154
of which outcrop samples	24	26	20	70
Total # of samples	109	135	167	411

Sample analysis

Samples were analyzed by X-ray fluorescence following standard protocols. To test the reproducibility of the analyses, four large samples were each split three ways, and independently prepared and measured by three different individuals. The pooled standard deviation of these 12 quality-control replicates provides our best estimate of the analytical uncertainty (which includes both measurement uncertainty and variability due to sample preparation). As Table 2 shows, the analytical uncertainty is a small percentage of the mean concentration of our field samples, except in the case of Th, for which the analytical uncertainty is 20% of the mean concentration. However, a more appropriate benchmark for comparison is the variability of the field samples one from another, as measured by their standard deviation. As the right-most column in Table 2 shows, the analytical uncertainty for most elements is 5-15% of the variability in our field samples. This implies that most of the variability we observe reflects real variability in the composition of our samples, rather than analytical variability due to sample preparation and measurement. A notable exception is Th, for which the analytical uncertainty is a large fraction of the variability observed in the field samples. Thus most of the variability in our measured values of Th appears to be noise rather than signal. For this reason, we will not analyze the Th data further.

Table 2. Reproducibility of XRF analyses

Element	analytical uncertainty (s.d. of quality control replicates)	mean of field samples	uncertainty as a fraction of mean	variability (s.d. of field samples)	uncertainty as a fraction of variability
Immobile elements (tracers for mass loss)					
Y (ppm)	0.54	11.75	5%	3.53	15%
Nb (ppm)	0.46	15.51	3%	3.10	15%
Th (ppm)	1.48	7.45	20%	1.95	76%
Zr (ppm)	2.19	126.10	2%	31.80	7%
TiO_2 (%)	0.0071	0.2708	3%	0.0791	9%
Mobile elements					
Na_2O (%)	0.051	3.480	1%	0.345	15%
MgO (%)	0.016	0.427	4%	0.139	12%
Al_2O_3 (%)	0.13	15.22	1%	0.84	15%
SiO_2 (%)	0.23	72.83	<1%	1.55	15%
P_2O_5 (%)	0.0023	0.0821	3%	0.0571	4%
K_2O (%)	0.029	3.345	1%	0.581	5%
CaO (%)	0.030	1.657	2%	0.356	8%
MnO (%)	0.00082	0.06384	1%	0.03483	2%
Fe_2O_3 (%)	0.058	1.589	4%	0.490	12%

Correlations among element concentrations

Sample-to-sample variations in element concentrations are correlated, reflecting differences in mineral abundances from one sample to the next. An example of these correlations is shown in Figure 1, which is a scatterplot matrix of concentrations in soils from watershed SC-2. As Figure 1 shows, the immobile tracers Zr and Ti are strongly correlated with each other and with Fe and Mg (and to a lesser extent with Al), suggesting that they co-occur in the mafic minerals. Nb, by contrast, is negatively correlated with Zr, Ti, Fe, and Mg but positively correlated with Na and K, suggesting that it occurs in association with feldspars. Y is weakly correlated with Nb and K, suggesting a weak association with K-spar.

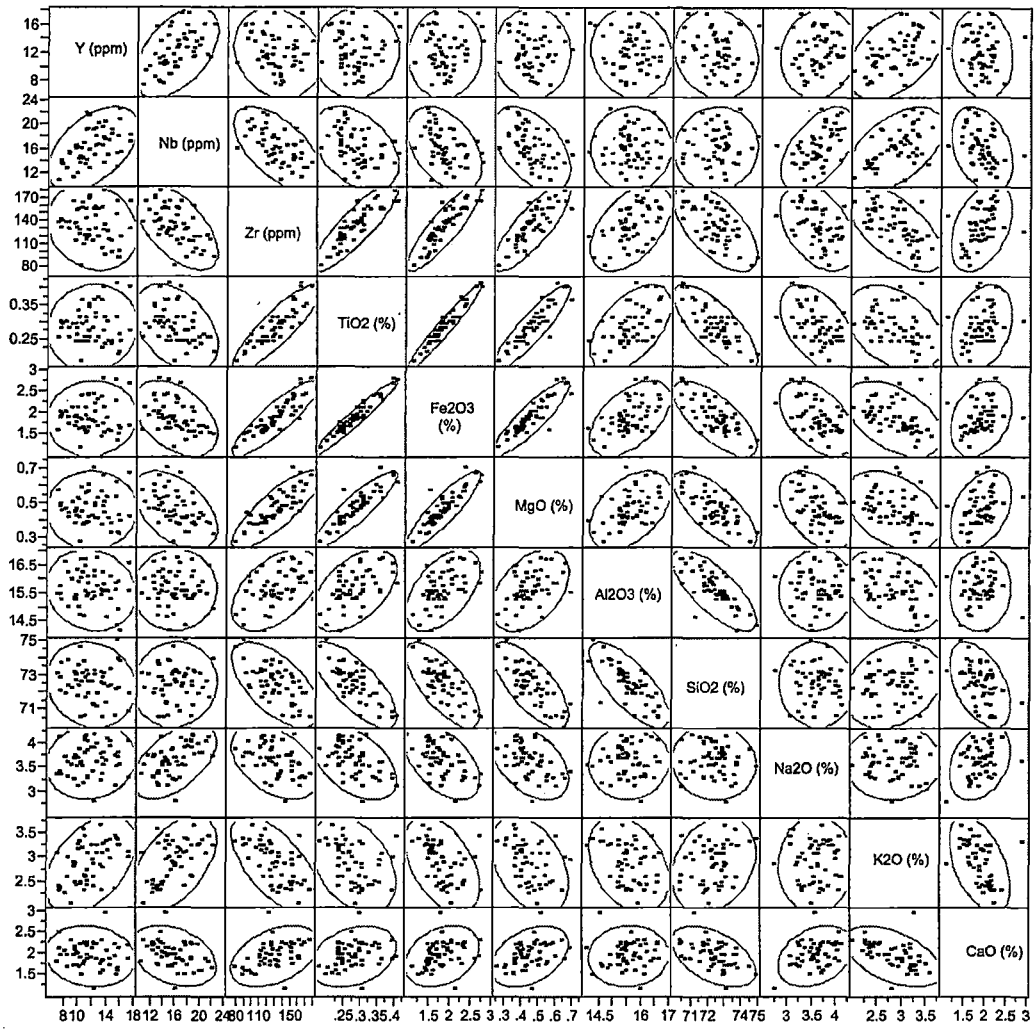

Figure 1. Scatterplot matrix for soil samples from watershed SC-2.

Similar correlations are observed in samples of parent material, but with more outlying points and larger ranges of variation reflecting greater sample-to-sample differences in mineral composition. This is consistent with the view that the soil undergoes a degree of homogenization associated with downslope creep and bioturbation.

There is significant risk of sampling bias in our samples of parent material, because rocks with some mineralogical compositions may be more likely than others to occur in outcrop (or as accessible saprolite under a thin soil cover), and therefore may be more likely to be sampled. We have attempted to correct for this sampling bias using the immobile tracers, using the following rationale.

As a volume of rock is converted to soil and the soil loses mass through chemical weathering, each of its immobile tracers should become enriched by the same ratio. Thus, the tracer concentrations in the rock and soil should be related by,

$$\frac{Y_{rock}}{Y_{soil}} \approx \frac{Nb_{rock}}{Nb_{soil}} \approx \frac{Zr_{rock}}{Zr_{soil}} \approx \frac{Ti_{rock}}{Ti_{soil}} \tag{4}$$

within the measurement uncertainties of the individual concentrations. Note that the ratios in equation (4) are same ratios that are used in equations (2) and (3) to partition the total denudation rate D into its two components, the physical erosion rate E and the chemical weathering rate W. To the extent that the different immobile tracers are enriched by markedly different ratios, they provide evidence that the soil was derived from parent material with a different composition from the rock that was sampled. Thus in calculating the average composition of the parent material in each catchment, we need to give greater weight to samples whose immobile tracer concentrations are more consistent (in the sense of equation 4) with the average soil. Note that this does not in any way specify what the enrichment ratio should be; it simply specifies that the enrichment ratios for each of the immobile tracers should be consistent with each other.

Our mathematical approach is derived from inverse variance weighting procedures used in maximum likelihood estimation. The mathematical details of our weighting procedure are as follows. We define the rock-to-soil ratio of a given immobile tracer, subscripted j, in an individual rock sample, subscripted i, as

$$f_{j,i} = \frac{C_{rock_{j,i}}}{< C_{soil_j} >} \tag{5}$$

where j=1, 2, 3, and 4 for Y, Nb, Zr, and Ti, $C_{rock_{j,i}}$ is the concentration of the j^{th} immobile tracer in the i^{th} individual rock sample, and $< C_{soil_j} >$ is the average concentration of that tracer in the soil. We define the average rock-to-soil tracer ratio for a given rock sample as the average of the ratios for each of its tracers,

$$\overline{f_i} = \frac{1}{4} \sum_{j=1}^{4} f_{j,i} \tag{6}$$

and the overall rock-to-soil ratio for the whole catchment as a weighted average of the individual rock samples,

$$F = \frac{\sum_{i=1}^{n} w_i \overline{f_i}}{\sum_{i=1}^{n} w_i} \tag{7}$$

where the weights w_i should be chosen so that the uncertainty in F is minimized. It can be shown that the uncertainty in a weighted average (here, F) is minimized if the weights w_i are the inverses of the variances

of the individual components being averaged (here, the $\overline{f_i}$). There are two different ways to estimate the variances (i.e., the squares of the uncertainties) in the individual $\overline{f_i}$. The first is by propagating the uncertainties in the concentrations $C_{rock_{j,i}}$ and $< C_{soil_j} >$ through equations 5 and 6. The second is from the variance of the $f_{j,i}$ values for each tracer in a given rock sample (which measures the overall degree of inequality in equation 4 above). If we pool these two estimates of variance, we obtain the following expression for the weights w_i:

$$w_i = \left[\frac{1}{12} \sum_{j=1}^{4} \left(f_{j,i} - \overline{f_i} \right)^2 + \frac{1}{16} \sum_{j=1}^{4} \left(f_{j,i} \frac{S_{Crock_{j,i}}}{C_{rock_{j,i}}} \right)^2 + \frac{1}{16} \sum_{j=1}^{4} \left(f_{j,i} \frac{S_{<C_{soil_j}>}}{< C_{soil_j} >} \right)^2 \right]^{-1} \quad (8)$$

where the first term accounts for the variance among the individual $f_{j,i}$ values, the second term propagates the uncertainty $S_{Crock_{j,i}}$ in the individual concentrations in the rock (estimated from the analytical uncertainty in Table 2), and the third term propagates the uncertainty $S_{<Csoil_j>}$ in the average concentration for the soil (estimated from the standard error of the mean soil concentration for each watershed, as shown in Table 3).

Immobile tracer concentrations and chemical denudation rates

Equations 2 and 3 show that we can use the enrichment of immobile tracers in soil, relative to parent material, to partition the total denudation rate D into its two components, the physical erosion rate E and the chemical weathering rate W. The results from this partitioning are shown in Table 3, which reveals three clear patterns.

The first clear pattern is that the rock-to-soil enrichment of Ti or Y is substantially larger than that of Nb or Zr. As a result, the chemical depletion fractions (the fraction of total mass loss that occurs through chemical weathering) implied by the Ti and Y concentrations are roughly 1.5 times greater than those implied by Nb or Zr. This pattern could be interpreted in at least three different ways. First, one could interpret these patterns as showing that Nb and Zr are significantly more mobile than Ti and Y. This seems improbable, since in these young soils all four tracers should be highly immobile, and one would expect Zr to be the least mobile of them all. A second possible interpretation is that mineral phases that contain Nb and Zr are being preferentially eroded, thus leaving behind soils that are relatively depleted in these tracer elements. This is unlikely, because the strong correlation between Zr and Ti (Figure 1) implies that they occur in association with the same minerals. The third interpretation, and the most probable one in our view, is that in spite of the weighting procedure we have used, the weighted average of the parent material samples is not fully representative of the parent material from which the average soil was derived.

Table 3: Immobile tracer concentrations and chemical denudation rates

Element & immobile reference element	Watershed SC-2	SC-5	SC-6
Immobile tracer concentrations			
Y (ppm)			
in parent material	9.3±0.4	8.3±0.4	10.3±0.7
in soil	12.0±0.4	11.4±0.2	13.5±0.3
Nb (ppm)			
in parent material	14.0±0.5	11.6±0.6	14.2±0.9
in soil	16.1±0.4	14.5±0.2	17.0±0.3
Zr (ppm)			
in parent material	111.9±4.0	118.4±5.6	105.5±7.0
in soil	131.5±3.2	151.0±3.1	126.2±2.0
Ti (wt % as TiO_2)			
in parent material	0.21±0.01	0.23±0.01	0.22±0.01
in soil	0.28±0.01	0.33±0.01	0.29±0.01
Chemical depletion fractions implied by immobile tracers:			
Y	0.23±0.04	0.27±0.04	0.23±0.05
Nb	0.13±0.04	0.20±0.04	0.16±0.05
Zr	0.15±0.04	0.22±0.04	0.16±0.06
Ti	0.26±0.03	0.31±0.04	0.25±0.04
Total denudation rate (D) from cosmogenic ^{10}Be (T km^{-2} yr^{-1}):			
	337±42	147±18	163±22
Chemical denudation rates (W in equation 2) from cosmogenic ^{10}Be and immobile tracers (T km^{-2} yr^{-1}): using immobile tracer:			
Y	77±17	39±7	38±10
Nb	43±12	29±7	26±9
Zr	50±14	32±7	27±10
Ti	86±16	45±8	41±9
11-yr mass balance	*13±1*	*12±1*	*10±1*

All values reported as means±standard errors. 11-year mass balances sum the of mass fluxes each element, converted to oxides to yield mass loss rates.

The second clear pattern in Table 3 is that our cosmogenic estimates of chemical weathering rates are typically 3-4 times higher than the chemical weathering rates measured by Clayton and Megahan

[1986] by input-output mass balance. One possible interpretation is that there is a systematic bias in one method or the other (or possibly both), although it is difficult to imagine a bias large enough to account for the difference. Another possible interpretation is that the average climatic and vegetation conditions, and thus the average weathering rates, may have differed substantially between the decade of the mass-balance measurements and the 5,000-12,000 yr time scale of our long-term measurements. This possibility needs to be investigated further, by calculating the magnitude of the climatic difference that would be required to account for the discrepancy in the weathering rate estimates. A third possible interpretation is that chemical weathering rates may exhibit episodicity, similar to (although smaller than) the episodicity in sediment yields inferred by Kirchner et al. [2001]. The mechanism underlying this hypothetical episodicity remains unclear. Forest fires elevate stream solute fluxes in the short term, but probably not elevated nearly enough to account for a 3-4-fold but probably not nearly enough to raise the long-term weathering rate by 3 or 4-fold. A fourth possible interpretation is that the immobile tracer concentrations may be artifactually enriched by atmospheric deposition of dust that is highly enriched in the immobile tracer elements. The plausibility of this hypothesis needs to be assessed, by estimating a reasonable rate of dust deposition and then calculating the tracer concentrations that this dust would need to have, in order to account for the enrichment in the soils. The fifth possible interpretation is that both measurements may be accurate, and the discrepancy between them may indicate that stream solute fluxes are partly decoupled from chemical weathering rates on hillslopes. One mechanism by which this could occur is the formation of secondary mineral phases in the stream, from solutes generated by weathering on the hillslopes. If these secondary minerals are large enough to be filtered out of water samples, they will not be counted as part of the solute flux in the stream even though they are produced from the chemical weathering flux from the hillslope. If this mechanism is at work, it could potentially be detected by comparing solute concentrations and fluxes in headwater channels with the solute concentrations and fluxes in the porewaters of their watersheds' hillslopes. It may also be possible to test for this mechanism using laboratory microcosm experiments.

The third clear pattern in Table 3 is that the cosmogenic denudation rate is roughly twice as high in watershed SC-2 as it is in watersheds SC-5 and SC-6. Because all of the chemical weathering rate calculations are scaled by the cosmogenic denudation rate, this translates directly into a factor of two in the cosmogenic estimates of weathering rates. One possibility is that the cosmogenic denudation rate estimates, which are based on a single cosmogenic analysis for each catchment, may simply be unreliable. We are now preparing new analyses of new cosmogenic samples to see whether we can replicate the earlier cosmogenic results. An alternative hypothesis is that the cosmogenic measurements are correct, and chemical weathering rates at SC-2 are indeed twice as high as those at SC-5 and SC-6. This seems unlikely in view of the remarkable consistency in the 11-year mass balances at the three watersheds.

Table 4: Mobile element concentrations in soil and parent material

Element	Watershed		
	SC-2	SC-5	SC-6
Na (wt % as element)			
in parent material	2.75±0.06	2.66±0.07	2.62±0.08
in soil	2.69±0.03	2.50±0.02	2.48±0.02
K (wt % as element)			
in parent material	2.73±0.12	3.03±0.09	3.06±0.09
in soil	2.37±0.05	2.67±0.03	2.82±0.02
Ca (wt % as element)			
in parent material	1.30±0.06	1.18±0.05	1.10±0.05
in soil	1.38±0.03	1.25±0.02	1.12±0.01
Mg (wt % as element)			
in parent material	0.20±0.02	0.21±0.01	0.21±0.02
in soil	0.28±0.01	0.32±0.01	0.28±0.01
Si (wt % as SiO_2)			
in parent material	73.69±0.75	73.97±0.39	73.52±0.31
in soil	72.41±0.14	71.77±0.15	72.52±0.13
Al (wt % as element)			
in parent material	7.74±0.11	7.66±0.11	7.83±0.10
in soil	8.26±0.04	8.28±0.05	8.12±0.04
Fe (wt % as element)			
in parent material	0.94±0.05	0.92±0.06	0.86±0.06
in soil	1.30±0.04	1.34±0.03	1.15±0.03

All values reported as means±standard errors

Mobile element concentrations and chemical weathering rates

Table 5 shows the chemical weathering rates inferred from equation 1 for each of the major mobile elements, using each of the immobile tracer elements to correct for rock-to-soil mass loss. We will briefly consider each of the elements in turn. We will focus on the results from watersheds SC-5 and SC-6, in view of the currently unresolved issues associated with the cosmogenic denudation rate measurement at watershed SC-2.

Sodium

Sodium appears to present the clearest test of the cosmogenic weathering rate calculations, because there should be relatively limited uptake of Na by vegetation, and relatively limited storage of Na by cation exchange in the watershed soils (though this needs to be checked with exchangeable cation measurements). In any case, the calculated long-term weathering rates for Na at SC-5 and SC-6 are the same, within error, as those measured with the 11-year mass balance.

Potassium

Potassium release from weathering, as estimated by the cosmogenic method, is roughly 8 times the net flux estimated by the 11-year input-output mass balance. One possibility is that growth in the watersheds' forests might have resulted in substantial potassium uptake during the decade of the mass balance measurements. The quantitative plausibility of this hypothesis needs to be assessed by estimating the likely growth rate of the forests and the resulting potassium uptake. Even if the forests were at steady state, it is still possible that potassium could be taken up into vegetation and then released from the watershed in the form of litter carried by the stream. Whether stream-borne litter fluxes could possibly account for the magnitude of the observed discrepancy (roughly 1 T km^{-2} yr^{-1}) would need to be quantitatively assessed.

Calcium

Long-term calcium fluxes estimated by the cosmogenic method are only one-third to one-half of the fluxes estimated from the 11-year input-output mass balance. Aeolian deposition of calcium-rich dust to the watersheds' soils could potentially raise the levels of calcium in the soils and thus depress the calculated long-term weathering fluxes. Alternatively, if atmospherically deposited calcium weathered quickly, it could raise calcium fluxes in streamflow above the weathering rate of the watersheds' parent material. Both of these possibilities need to be assessed by reviewing the literature on aeolian deposition. The discrepancy in the fluxes could also potentially arise from the weathering of trace amounts of calcite from the granite at depth, such that the bedrock surface could already be depleted of calcium when we sample it as the parent material. This hypothesis would imply that the granite initially consisted of roughly 0.3% calcium in the form of calcite; the plausibility of this would need to be assessed.

Magnesium

Magnesium is just as enriched in the soils as the immobile tracers are, yielding a weathering rate near zero by the cosmogenic method. By contrast, the 11-year mass balance yields a clear, though not particularly large, magnesium flux from weathering. As with calcium, both atmospheric deposition and deep weathering of the bedrock are possible explanations that need to be assessed. The Silver Creek

watersheds may also contain basaltic dikes, and occasional basalt hand-samples were found along the eastern boundary of watershed SC-2. Weathering of small amounts of basalt could potentially release enough magnesium to account for the discrepancy between the cosmogenic and mass balance calculations.

Table 5: Base cations: long-term vs. short-term chemical denudation rates (T km^{-2} yr^{-1})

Element & immobile reference element	Watershed SC-2	Watershed SC-5	Watershed SC-6
Na weathering flux (T km^{-2} yr^{-1} as element)			
Y	2.29±0.48	1.21±0.20	1.17±0.27
Nb	1.36±0.40	0.96±0.20	0.89±0.24
Zr	1.56±0.40	1.02±0.20	0.90±0.26
Ti	2.51±0.45	1.35±0.22	1.24±0.25
11-yr mass balance	*1.33±0.13*	*1.16±0.10*	*1.24±0.15*
K (T km^{-2} yr^{-1} as element)			
Y	3.04±0.52	1.58±0.24	1.46±0.31
Nb	2.23±0.44	1.31±0.23	1.13±0.28
Zr	2.40±0.44	1.37±0.23	1.14±0.31
Ti	3.24±0.50	1.72±0.26	1.53±0.29
11-yr mass balance	*0.17±0.03*	*0.19±0.04*	*0.17±0.04*
Ca (T km^{-2} yr^{-1} as element)			
Y	0.81±0.23	0.38±0.08	0.39±0.11
Nb	0.33±0.20	0.26±0.09	0.26±0.10
Zr	0.43±0.20	0.29±0.08	0.26±0.11
Ti	0.92±0.21	0.45±0.09	0.42±0.10
11-yr mass balance	*1.82±0.20*	*1.01±0.13*	*0.86±0.13*
Mg (T km^{-2} yr^{-1} as element)			
Y	-0.04±0.04	-0.03±0.02	-0.01±0.03
Nb	-0.13±0.05	-0.06±0.02	-0.04±0.03
Zr	-0.11±0.04	-0.05±0.02	-0.04±0.03
Ti	-0.01±0.04	-0.01±0.02	-0.01±0.02
11-yr mass balance	*0.15±0.01*	*0.12±0.02*	*0.13±0.02*

All values reported as means±standard errors

Table 5 (cont'd): Si, Al, and Fe: long-term vs. short-term chemical denudation rates (T km^{-2} yr^{-1})

Element & immobile reference element	Watershed SC-2	SC-5	SC-6
Si (T km^{-2} yr^{-1} as SiO_2)			
Y	60.40±12.70	31.55±5.46	29.21±7.45
Nb	35.52±10.41	24.28±5.38	20.85±6.69
Zr	40.78±10.38	26.01±5.32	21.08±7.36
Ti	66.53±11.89	35.46±5.82	31.13±6.75
11-yr mass balance	*7.96±0.82*	*8.71±0.96*	*7.04±0.87*
Al (T km^{-2} yr^{-1} as element)			
Y	4.65±1.31	2.36±0.53	2.61±0.79
Nb	1.81±1.10	1.52±0.55	1.67±0.72
Zr	2.41±1.08	1.72±0.54	1.70±0.80
Ti	5.35±1.18	2.81±0.57	2.82±0.71
11-yr mass balance	*0.0048±0.0006*	*0.0076±0.0011*	*0.0073±0.0011*
Fe (T km^{-2} yr^{-1} as element)			
Y	-0.20±0.21	-0.08±0.08	-0.04±0.11
Nb	-0.64±0.21	-0.21±0.09	-0.17±0.11
Zr	-0.55±0.20	-0.19±0.09	-0.45±0.14
Ti	-0.09±0.18	-0.01±0.08	-0.17±0.12
11-yr mass balance	*0.02±0.004*	*0.04±0.01*	*0.05±0.01*

All values reported as means±standard errors

Silicon

Because SiO_2 accounts for most of the mass of the soil and parent material, the results reported above for the overall chemical denudation rate mirror the results shown for SiO_2 in Table 5. Weathering fluxes of SiO_2 estimated by the cosmogenic method are approximately 3-4 times those estimated from the 11-year mass balance. Several possible explanations for this discrepancy are mentioned above in the discussion of the overall denudation rate. A further possibility that needs to be examined is that minerals that are higher than average in SiO_2 (such as large quartz and feldspar grains derived from pegmatites) could potentially be preferentially eroded if they became concentrated at the surface, for example through winnowing associated with freeze-thaw or bioturbation processes. In this case, immobile tracer elements that are not associated with high-silicon minerals would be preferentially enriched in the soil that was left behind. The net result would be that what was actually an erosional flux of SiO_2 would artifactually appear to be a weathering flux. However, whether one uses Zr and Ti (which are associated with low-SiO_2 samples) or Y and Nb (which are uncorrelated with SiO_2), one obtains similar weathering fluxes of

SiO_2 from the cosmogenic method, suggesting that preferential erosion is unlikely to be the cause of the discrepancy with the 11-year mass balance.

Aluminum

Aluminum fluxes from the 11-year mass balance are nearly zero, reflecting the very low solubility of aluminum under the pH conditions that characterize the streams. Conventionally, the absence of aluminum in streamflow is attributed to formation of secondary minerals. However, if the cosmogenic calculations are approximately correct, they imply that there is substantially less Al in the soils than in the rocks from which they were derived (after correcting for mass loss using the immobile tracers). This could potentially be explained by Al-rich secondary minerals being precipitated in or near the stream, and carried from the watershed as sediment rather than solutes. The implication of this hypothesis is that soil porewaters should have elevated Al concentrations, compared to the streamwaters that they ultimately become. This prediction is potentially testable through field measurements.

Iron

The watershed soils are more enriched in iron than in the immobile tracer elements, leading equation 1 to infer negative iron weathering rates. This result could arise if iron-poor minerals are preferentially eroded from the soil surface (see the discussion of SiO_2 above), or if an iron-rich parent material (such as basaltic dikes) has been under-sampled.

References

April, R., R. Newton, and L. T. Coles, Chemical weathering in two Adirondack watersheds: Past and present-day rates, *Geological Society of America Bulletin,* **97**, 1232-1238, 1986.

Brimhall, G. H., O. A. Chadwick, C. J. Lewis, W. Compston, I. S. Williams, K. J. Danti, W. E. Dietrich, M. E. Power, D. Hendricks, and J. Bratt, Deformational mass-transport and invasive processes in soil evolution, *Science,* **255**, 695-702, 1992.

Brown, E. T., R. F. Stallard, M. C. Larsen, D. L. Bourles, G. M. Raisbeck, and F. Yiou, Determination of pre-development denudation rates of an agricultural watershed (Cayaguas River, Puerto Rico) estimated from in-situ-produced ^{10}Be in river-borne quartz, *Earth and Planetary Science Letters,* **160**(3-4), 723-728, 1998.

Clayton, J. L., and W. F. Megahan, Erosional and chemical denudation rates in the southwestern Idaho batholith, *Earth Surface Processes and Landforms,* **11**, 389-400, 1986.

Kirchner, J. W., R. C. Finkel, C. S. Riebe, D. E. Granger, J. L. Clayton, J. G. King, and W. F. Megahan, Mountain erosion over 10-year, 10 000-year, and 10 000 000-year timescales, *Geology*, in press, 2001.

Lal, D., Cosmic ray labeling of erosion surfaces: In situ nuclide production rates and erosion models, *Earth and Planetary Science Letters,* **104**, 424-439, 1991.

Riebe, C. S., J. W. Kirchner, D. E. Granger, and R. C. Finkel, Strong tectonic and weak climatic control of long-term chemical weathering rates, *Geology,* **29**, 511-514, 2001.

White, A. F., A. E. Blum, M. S. Schulz, D. V. Vivit, D. A. Stonestrom, M. Larsen, S. F. Murphy, and D. Eberl, Chemical weathering in a tropical watershed, Loquillo mountains, Puerto Rico: 1. Long-term versus short-term weathering fluxes, *Geochimica et Cosmochimica Acta,* **62**(2), 209-226, 1998.